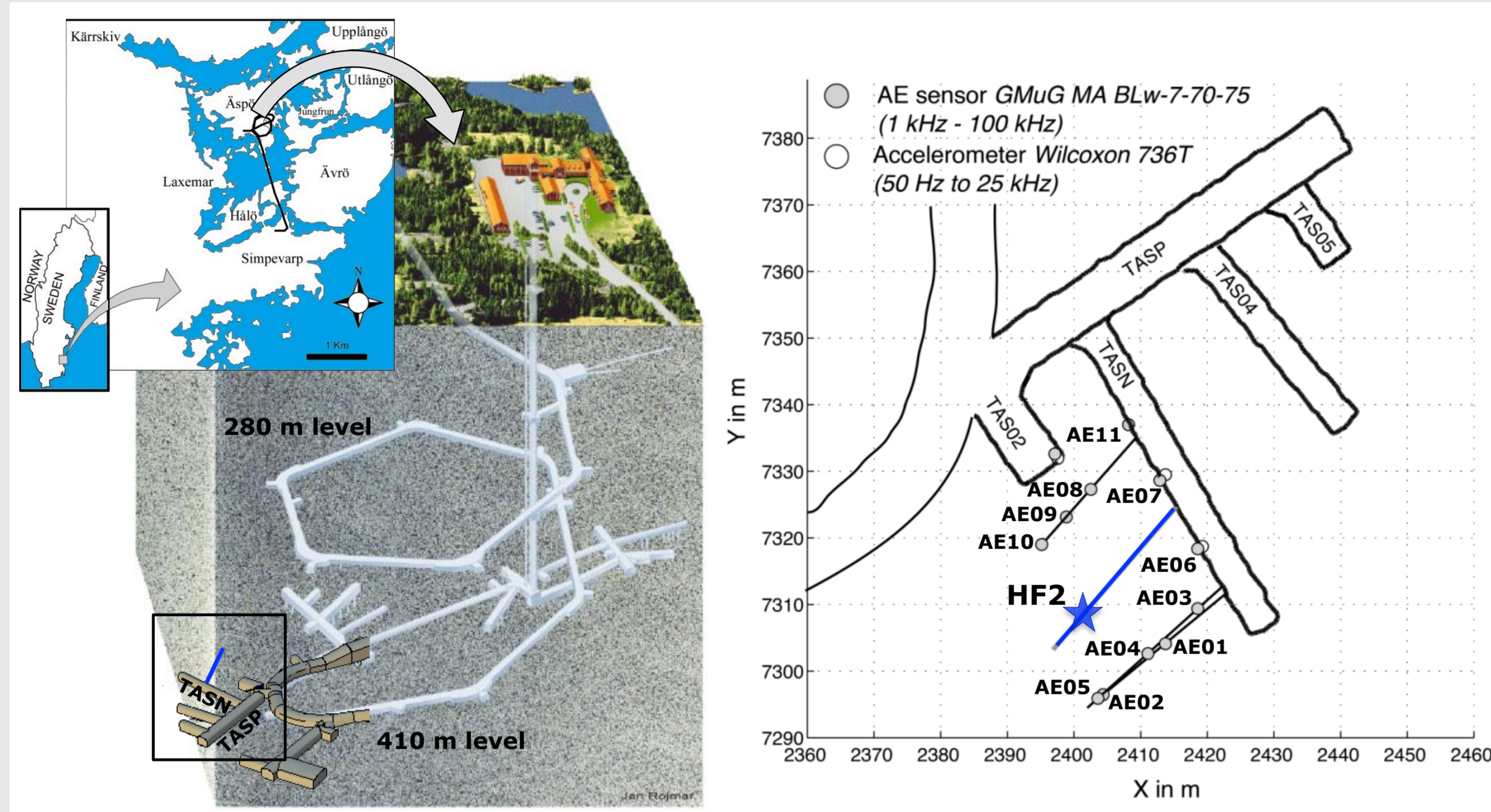


# GFZ Automated detection and location of picoseismicity of hydraulic fracturing experiment using continuous waveforms

## 1. INTRODUCTION

An in situ hydraulic fracturing experiment was performed at Äspö Hard Rock Laboratory (Sweden) aiming at optimizing geothermal heat exchange in crystalline rock mass (Zang et al. 2016). A near field network with 11 acoustic emission (AE) sensors was installed 410 m below surface to map the seismic response of hydraulic fractures for different fluid injection scenarios (Figure 1). The basic idea of the experiment was to compare hydraulic fracturing growth and induced seismicity under controlled conditions in a horizontal borehole 30 meter long for conventional fluid injection versus cyclic fluid injection, and dynamic pulse hydraulic fracturing (Zang et al., 2016). The piezo-electric sensors have their highest sensitivity in the frequency range 1 to 100 kHz. Sampling rates were extended to 1 MHz. The acquisition system was capable to operate in trigger and continuous mode. In this poster, we present the results obtained during the conventional, continuous water-injection experiment HF2 (Hydraulic Fracture 2), and discuss the detection performance using a recently developed automated full waveform detection algorithm.



**Figure 1.** Test site for hydraulic fracturing in an experimental tunnel of Äspö Hard Rock Laboratory, Sweden (top). Sensors are employed in the near-field (bottom): a blue line indicates the hydraulic testing borehole, the blue star identifies the fluid injection segment corresponding to the HF2 experiment.

## 2. AUTOMATED FULL WAVEFORM DETECTION (LASSIE)

We consider continuous recordings and apply a recently developed automated full waveform detection and location algorithms (Lassie, <https://gitext.gfz-potsdam.de/heimann/lassie>, Heimann et al., 2016). This friendly earthquake detector is based on the stacking of smooth characteristic functions calculated from normalized amplitude envelopes (Figure 2). A visual inspection of seismic waveforms reveals different kinds of detected signals that we have classified as: acoustic emission (AE) detections, false detections, electronic noise, anthropogenic noise, long period noise and other signals (figure 3 and 4).

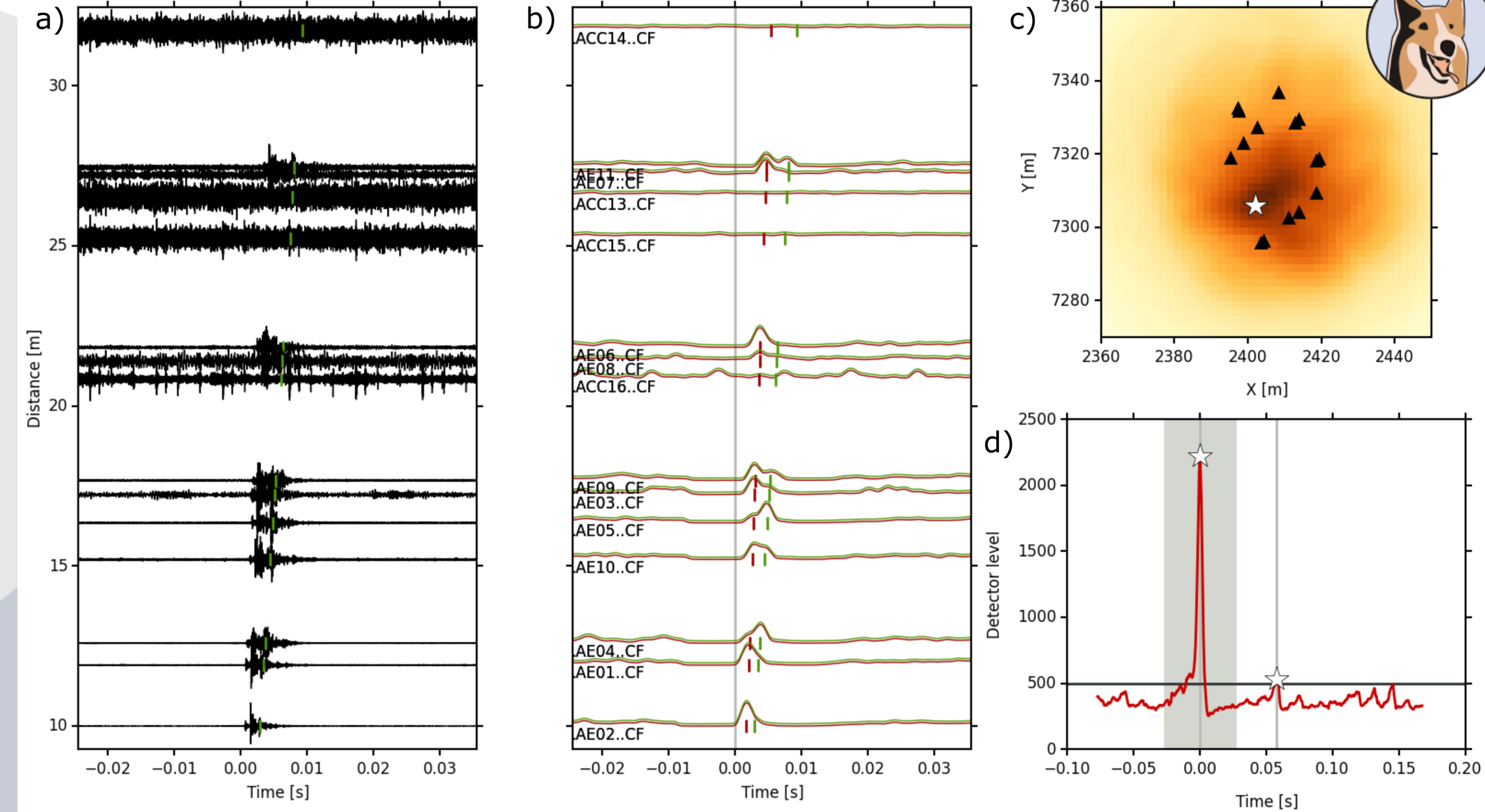


**Figure 2.** Example of acoustic emission detection (the origin time is 08:35:24.477). a) Waveforms sorted by hypocentral distance. b) Characteristic function (normalized amplitude envelopes) for each trace. These are used for travel-time stacking corrected with P-wave speed (red lines) and S-wave speed (green lines). The markers indicate the (best-fit) synthetic arrival time of the respective phases at each sensor. c) Coherence (stack) map for the search region. Dark colors denote high coherence values. The location of the detected event is marked by a white star. Sensor locations are shown with black triangles. d) Global detector level function in a processing time window from -0.1 to +0.2 seconds around the origin time of the detected event. The cut-out time window used for the coherence map is shown in gray color. White stars indicate this and other detection within the same processing time window, exceeding a detector level threshold of 500.

## 3. DETECTION PERFORMANCE

The highest rates of acoustic emission detections are found during the fluid injection stages (figure 4a). A low detector threshold is chosen not to lose weak events. However, a large number of false detections is also found (figure 4b). Electronic noise is found associated with the fluid injection stages and hinders the search of real events requiring a posteriori classification. Anthropogenic noise, long period and other signals are also detected and distributed through the whole experiment. For such cases, the values of amplitude of the characteristic function are usually low (see examples in figure 3).

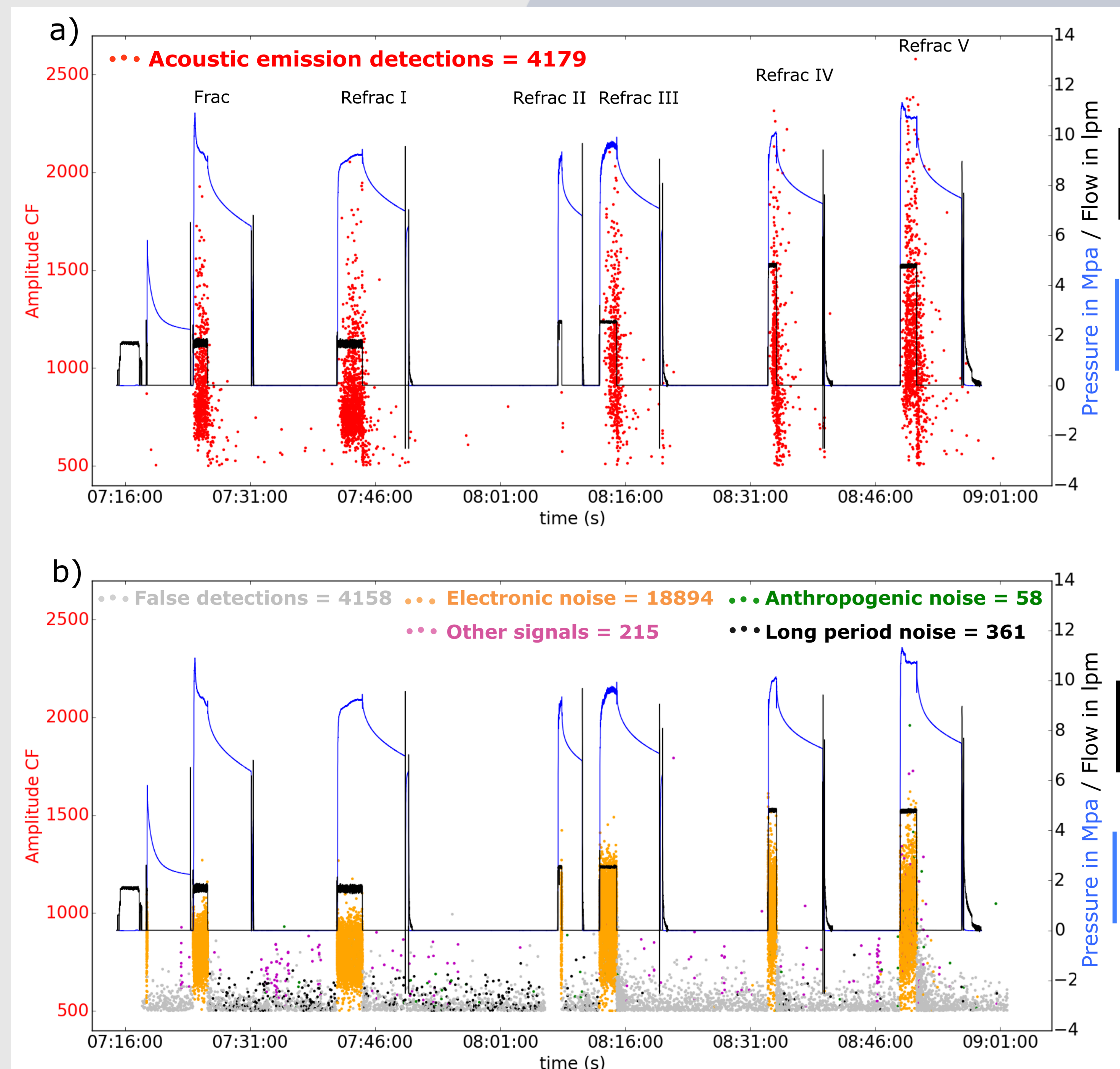


**Figure 4.** a) Acoustic emission detections using continuous recordings. b) Other kinds of detected signals from a visual inspection that do not correspond with seismic events. Amplitude of the characteristic function (left ordinate), injection pressure and flow rate (right ordinate) for hydraulic fractures in the experiment HF2 are shown.

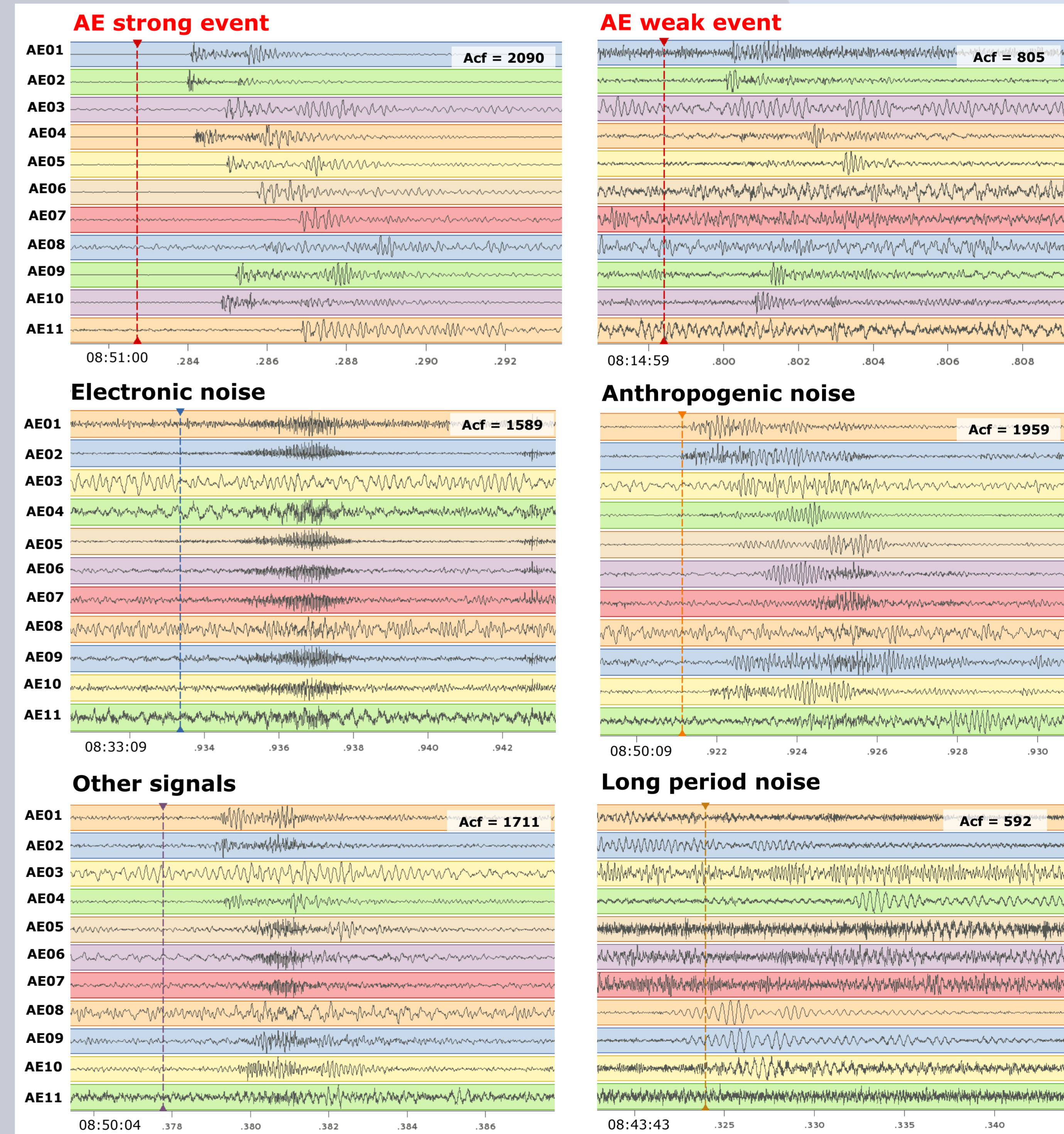


**Figure 3.** Events detected by the Lassie algorithm (Heimann et al. 2016) during HF2, showing timing and amplitude of the characteristic function (Acf). Waveforms are band-pass filtered in the frequency range 3 – 70 kHz. The time (ms) is shown on the x-axis and the reference time is displayed in the lower left corner of each box.

## 4. CONCLUSIONS

- A detector based on the stacking of smooth characteristic functions can be successfully used to detect AE signals for massive datasets with large number of sensors and/or extremely high sampling (here 1 MHz); our results supports the adoption of similar techniques for other induced and natural seismic activity monitoring systems.
- The choice of detection threshold influences the detection performance. A low threshold allows the detection of weak events at the cost of a higher number of false detection.
- The detection setup can be combined with a classification algorithm (here we showed results of a visual classification) to distinguish true and false events, and classify different signals.
- The posterior waveform analysis illustrates that noise from different anthropogenic processes is found during fracking operations.

## REFERENCES & ACKNOWLEDGEMENTS

Zang A., O. Stephansson, L. Stenberg, K. Plenkers, C. Milkereit, G. Kwiatek, G. Dresen, E. Schill, G. Zimmermann, T. Dahm and M. Weber (2016). The geothermic fatigue hydraulic fracturing experiment at Äspö Hard Rock Laboratory, Sweden – Monitoring design, hydraulic testing and first results, *Geophys. J. Int.*, under review.

Heimann S., C. Matos, S. Cesca, I. Rio and S. Custodio (2016). Lassie: A versatile tool to detect and locate seismic activity, *Seismological Research Letters*, in preparation.

Note: interested users to preview Lassie can write to: [sebastian.heimann@gfz-potsdam.de](mailto:sebastian.heimann@gfz-potsdam.de)

This work is funded by the EU H2020 SHEER project ([www.sheerproject.eu](http://www.sheerproject.eu)). Nova project 54-14-1 was financially supported by the GFZ German Research Center for Geosciences (75%), the KIT Karlsruhe Institute of Technology (15%) and the Nova Center for University Studies, Research and Development (10%). An additional in-kind contribution of SKB for using Äspö Hard Rock Laboratory as test site for geothermal research is greatly acknowledged.